Acta Geochim
https://doi.org/10.1007/s11631-020-00424-4

ORIGINAL ARTICLE

Genesis of the Maoping carbonate-hosted Pb–Zn deposit, northeastern Yunnan Province, China: evidences from geology and C–O–S–Pb isotopes

Yufan He[1,2] · Tao Wu[1,2] · Zhilong Huang[1] · Lin Ye[1] · Ping Deng[3] · Zhenzhong Xiang[1,2]

Received: 19 June 2020 / Revised: 13 July 2020 / Accepted: 27 July 2020

Abstract The Maoping Pb–Zn deposit (~ 3 Mt Pb + Zn reserves with grades of 12–30 wt%) is one of the largest Pb–Zn deposits in the Sichuan–Yunnan–Guizhou (SYG) metallogenic province, which has contributed a tremendous amount of lead and zinc resources for China. To obtain a further understanding of the sources of ore-forming materials and ore genesis of the deposit, S–Pb isotopes of sulfides and C–O isotopes of ore-stage calcites were systematically collected from representative orebodies at different elevations with a Finnigan MAT-253 mass spectrometer. The calcites separated from the sulfides of the No I and No II orebodies shared identical $\delta^{13}C_{PDB}$ values (− 5.3 to − 0.8 ‰) and $\delta^{18}O_{SMOW}$ values (+ 14.5 to + 21.8 ‰) with those of the calcites in the SYG region, suggesting that CO_2 in regional ore-forming fluids possibly had a homologous C–O source that originated from a ternary mixture of the dissolution of marine carbonate rocks, degassing process of the Emeishan mantle plume, and dehydroxylation of sedimentary organic matter. The No. I-1 and No. I-2 orebody was hosted in the same strata, but the sulfur source of No. I-1 orebody (+ 13.1 to + 19.0 ‰) with equilibrated sulfur fractionation ($\delta^{34}S_{sphalerite} < \delta^{34}S_{galena}$) and No. I-2 orebody (+ 18.0 to + 21.8 ‰) with sulfur equilibrium fractionation ($\delta^{34}S_{sphalerite} > \delta^{34}S_{galena}$) were different. They were derived from the allopatry thermochemical sulfate reduction (TSR) of overlying Carboniferous sulfates in the ore-hosting strata and local TSR of sulfates in the ore-bearing Upper Devonian Zaige Formation, respectively. The narrow and uniform Pb isotopic ratios of single galena grains collected from sulfides with $^{206}Pb/^{204}Pb$ of 18.713–18.759, $^{207}Pb/^{204}Pb$ of 15.772–15.776 and $^{208}Pb/^{204}Pb$ of 39.383–39.467 indicate a well-mixed metal source(s) that consist of Proterozoic Kunyang and Huili Group basement rocks and Devonian to Middle Permian ore-hosting sedimentary rocks. Besides, the late Permian Emeishan basalts are difficult to contribute metals for regional Pb–Zn mineralization despite a closely spatial relationship with the distribution of the Pb–Zn deposit. This is supported by Pb isotopic ratios plotting above the average upper crustal Pb evolution curves and staying far away from that of the age-corrected Emeishan basalts. Hence, taking into account of the similarities in tectonic setting, ore-hosting rock, ore assemblage, wall rock alteration, ore-controlling structure, and ore-forming materials and the differences in relationship with regional magmatism, fluid inclusion characteristic and ore grade between the Maoping deposit and typical MVT Pb–Zn deposit, the ore genesis of the Maoping deposit should be an MVT like Pb–Zn deposit.

Keywords Maoping Pb–Zn deposit · Ore-forming materials · Ore genesis · MVT-like deposit

✉ Tao Wu
wutao@mail.gyig.ac.cn

[1] State Key Laboratory of Ore Deposit Geochemistry, Institute of Geochemistry, Chinese Academy of Sciences, Guiyang 550081, China

[2] University of Chinese Academy of Sciences, Beijing 100049, China

[3] Yiliang Chihong Mining Co., Ltd., Zhaotong 657000, China

1 Introduction

The Sichuan–Yunnan–Guizhou (SYG) Pb–Zn metallogenic province, including the southern Sichuan, northeastern Yunnan and northeastern Guizhou ore districts, is located in the southwestern Yangtze block (Fig. 1a; Huang

Published online: 04 August 2020

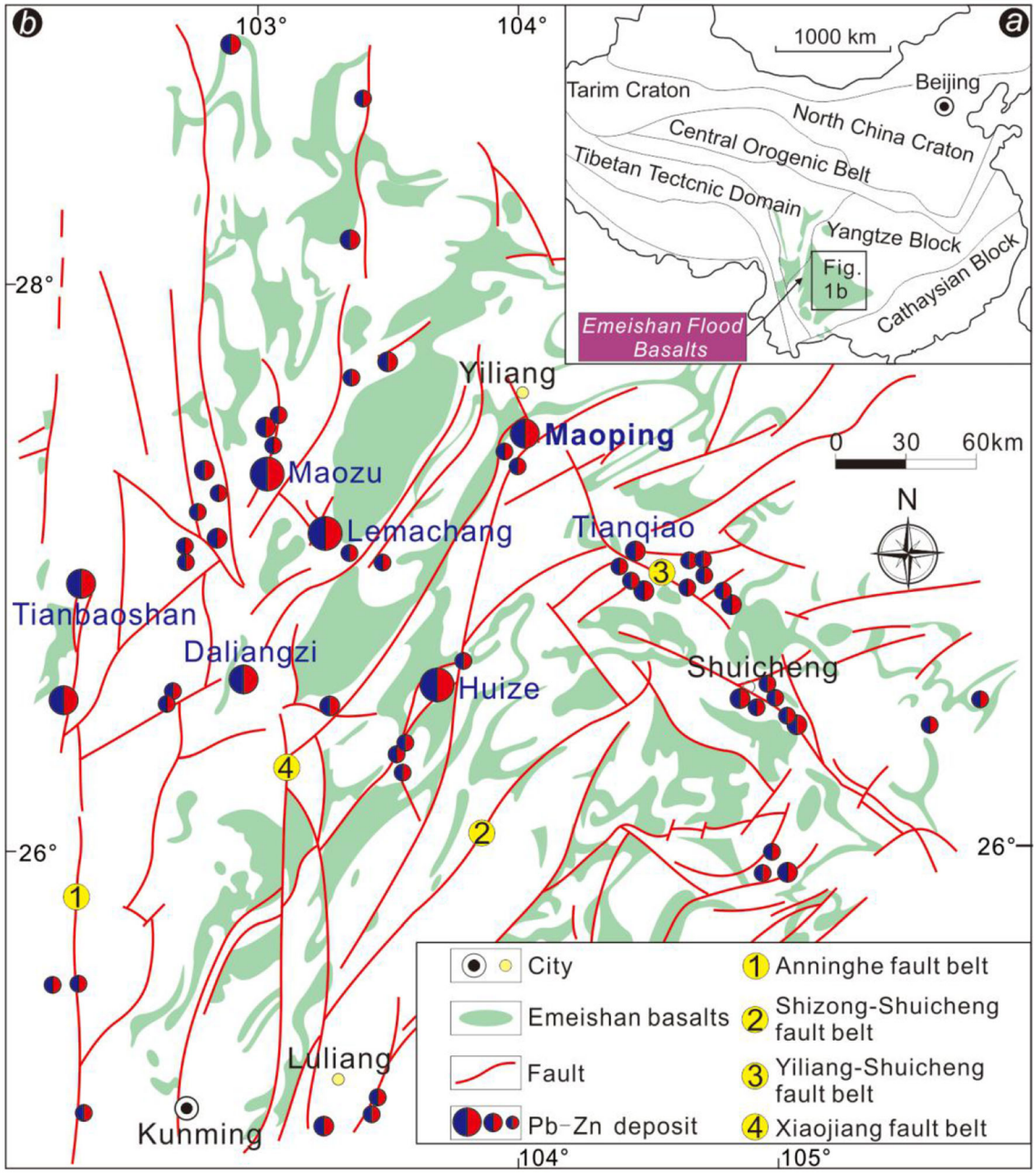

Fig. 1 Geological sketch map of the Sichuan–Yunnan–Guizhou (SYG) Pb–Zn metallogenic province, showing the Geotectonic location (**a**) and the distribution of faults, Emeishan flood basalts and Pb–Zn deposits (**b**, modified after Liu and Lin 1999)

et al. 2004; Zhang et al. 2005), which is a significant part of the giant South China low-temperature metallogenic domain (SCLTMD) and also an important production base of lead, zinc, germanium, and silver in China (Hu et al. 2016, 2017a, b; Zhou et al. 2018). Several world-class to large-scale Pb–Zn deposits occur in the northeastern Yunnan district under a similar metallogenic setting, such as Huize, Lemachang, Maoping, Fule, Maozu, and Jinshachang, etc. (Fig. 1b; Ye et al. 2011; Han et al. 2012; Zhou et al. 2013a, 2018). These deposits are characterized by (1) being hosted in the carbonate rocks of the late Ediacaran to middle Permian strata (Zhou et al. 2018); (2) being controlled by multi-stage faults and spatially relevant to the late Permian Emeishan basalts (Fig. 1b; Han et al. 2012; Wang et al. 2017); (3) having stratiform, lenticular and scrotiform sulfide orebodies with significant epigenetic features occurred in the fold bedding-planes or steep sulfide veins displayed along fault dip planes (Zheng and Wang 1991; Li et al. 2015; Wei et al. 2015); (4) having low-moderate temperature (120–280 °C) and medium–

high salinity (10–22 wt% NaCl equiv.) of the fluid inclusions (Zhang et al. 2015; Liu et al. 2017); and (5) having high ore grades with 10–35 wt% Pb + Zn and associated with Ge, Ag, Cd and Ga, etc. (Zhou et al. 2014a; Zhu et al. 2017).

The Maoping deposit is the second largest Pb–Zn deposit in the SYG region with more than three million tons (Mt) of lead and zinc reserves (Tan et al. 2019), which is just second to the world-class Huize deposit (> 5 Mt Pb + Zn reserves; Huang et al. 2004). During the past decades, great progresses have been made in geological features (Wei et al. 2015; Wang et al. 2017), fluid inclusions (Han et al. 2007; Wang et al. 2009; Cui and Han 2014), associated elements (Qiu et al. 2013; Chen et al. 2016), sphalerite Rb–Sr dating (Shen et al. 2016; Yang et al. 2019), and S–Pb isotopic studies (Ren et al. 2018; Tan et al. 2019; Xiang et al. 2020) in Maoping deposit. However, the Maoping deposit had received a little attention of research, especially on the metallogenic age, source(s) of ore-forming materials, and relationship between Emeishan basaltic magmatism and regional Pb–Zn mineralization. Several aspects of the ore genesis are still under debate. For example, Shen et al. (2016) obtained a sphalerite Rb–Sr isochron age of 321.7 ± 5.8 Ma, while a younger sphalerite Rb–Sr isochron age of 202.5 ± 8.5 Ma was reported by Yang et al. (2019). Furthermore, according to the research of C–H–O isotopes, the ore-forming fluids were mainly derived from magma and hosted formation waters with a certain contribution from metamorphic water (Zou et al. 2004; Han et al. 2007). However, based on the analyses of S-Pb isotopes, the ore-forming metals were mainly originated from ore-bearing rocks with the addition of some basements and basalt components (Tan et al. 2019; Xiang et al. 2020). Besides, it is still disputable on whether most epigenetic Pb–Zn deposits in the SYG region, including the Maoping deposit, can be classified as the Mississippi Valley-type (MVT) Pb–Zn deposit (Han et al. 2007; Zhang et al. 2019a, b; Luo et al. 2020).

Previous studies have proven that C–O–S–Pb isotopic analyses are powerful means to determine the source(s) of ore-forming fluid and constrain the origin of the ore deposit (Li et al. 2015; Zhou et al. 2013a; Tan et al. 2017; Wang et al. 2018; Luo et al. 2020). In this study, based on the detailed ore deposit characteristics, systematic C–O isotopes of ore-stage calcites from No. I and II orebodies and comprehensive S–Pb isotopes of sulfides in No. I orebody (group) from bottom to top with exact elevations are collectively investigated to trace the carbon, oxygen, sulfur, and metal source(s) and discuss the ore genesis of the Maoping Pb–Zn deposit. The outcomes will provide further understanding of the formation of the SYG Pb–Zn metallogenic province and similar deposits in the SCLTMD.

2 Geological setting

The SYG Pb–Zn metallogenic province is situated in a triangle area enclosed by NS-trending Anninghe fault, NE-trending Shizong-Mile fault and NW-trending Yiliang-Shuicheng fault (Fig. 1b; Ren et al. 2018). The regional stratigraphy is mainly composed of Archean to Paleoproterozoic crystalline basements, Meso- to Neoproterozoic folded basements, and cover sequences that consist of Paleozoic to Early Mesozoic marine sedimentary rocks, Late Permian Emeishan continental flood basalt and Late Mesozoic to Cenozoic continental sedimentary rocks (Tan et al. 2019; Zhang et al. 2019a, b). Folds and faults widely occurred in the SYG region due to multi-stage tectonic movements including Caledonian, Hercynian, Indosinian and Yanshanian periods (Liu and Lin 1999). At about 260 Ma, large-scale mantle-plume-related magmatic activities took place, which formed widely distributed Emeishan basalts covering an area of over 250,000 km^2 (Fig. 1b; Zhou et al. 2002). Almost all Pb–Zn deposits of the SYG area are spatially located in the Emeishan Large Igneous Province (ELIP) (Fig. 1b; Liu and Lin 1999; Cui and Han 2014; Huang et al. 2004, 2010).

The Maoping Pb–Zn deposit is located in the northeastern SYG in Zhaotong City, Yunnan province, South China (Fig. 1a, b). Within the ore district, exposed strata mainly include the Silurian to Triassic marine sedimentary rocks (Fig. 2). Among which, the dolostone and limestone of the Upper Devonian Zaige Formation (D_3zg), Lower Carboniferous Baizuo Formation (C_1b), and Middle Carboniferous Weining Formation (C_2w) are the most significant ore-hosting rocks (Fig. 3, Xiang et al. 2020). The NW-trending fault group including Fangmaba, Maoping, and Tuogumei faults collectively controlled the distribution of the Pb–Zn deposits in the region. Most orebodies, occurring as a ladder shape on the profile (Fig. 3), have a clear boundary with carbonate wall rocks (Fig. 4b). These stratoid, lenticular and veined orebodies (No. I, II, and III) of the Maoping deposit, yielding more than 3 Mt Pb + Zn resources at grades of 12–30 wt% (Ren et al. 2018), are hosted in the interlayer fracture zone in the steeply inclined strata of the Maomaoshan anticline (Figs. 3, 4a–c) and structurally controlled by NE-trending Maoping fault (Fig. 2; Liu and Lin 1999). The No. I orebody (group) can be further divided into No. I-1 and I-2 orebody, hosted in the dolostone and limestone of the Upper Devonian Zaige Formation, which is the largest orebody with the most abundant Pb–Zn resources grading at 20–45 wt% Pb + Zn in the Maoping deposit.

Ore types of the Maoping deposit can be divided into sulfide and oxidized ores, which were formed in the hydrothermal and supergene ore-stage, respectively. Ore

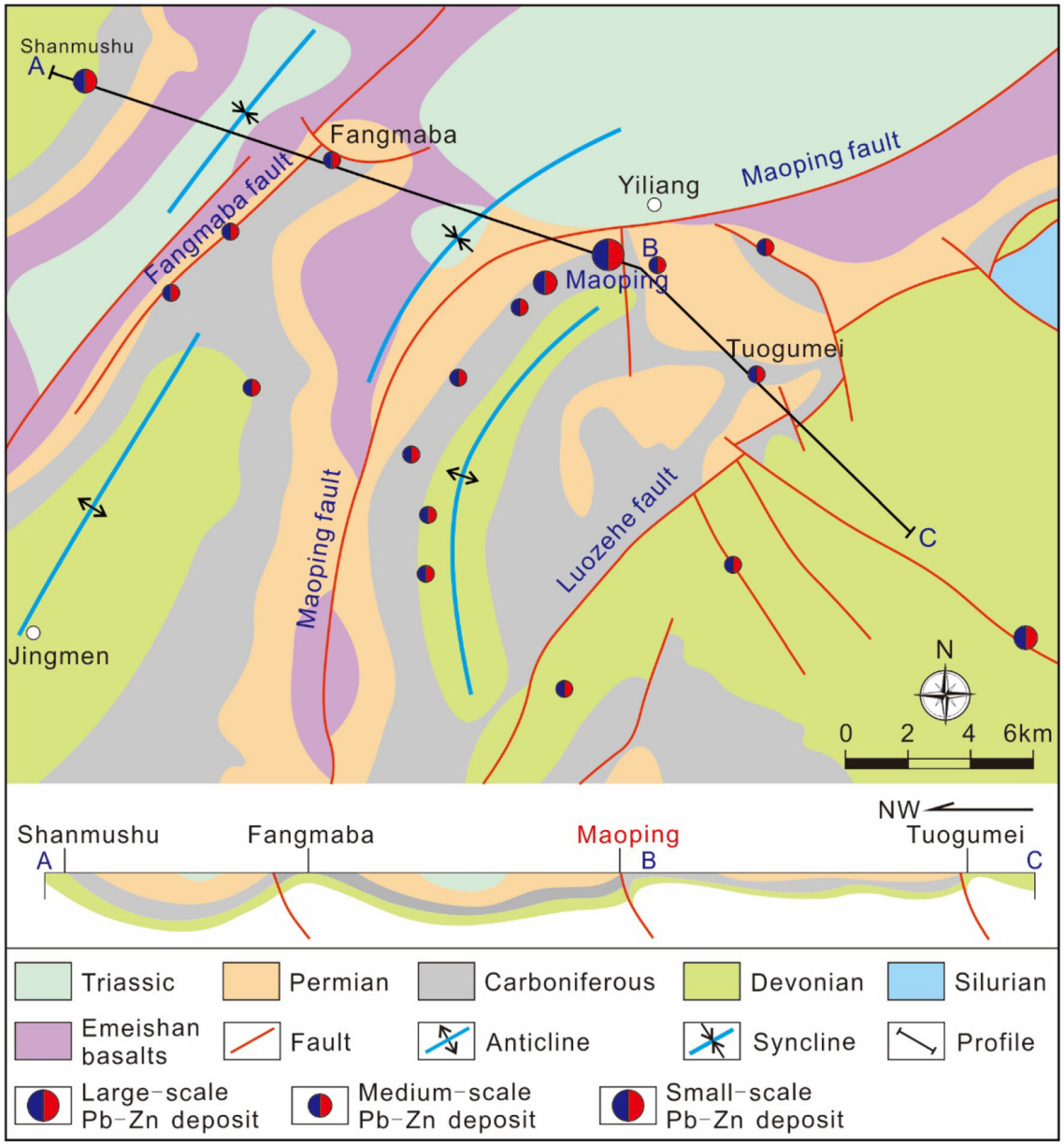

Fig. 2 Geological sketch map of the Maoping Pb–Zn deposit, displaying the A–B–C profile and the distribution of the strata, faults, and surrounding Pb–Zn deposits. Modified after Liu and Lin (1999)

minerals of sulfides include sphalerite, galena, pyrite and minor chalcopyrite (Fig. 4d–f). The major gangue minerals are dolomite (Fig. 4b), calcite (Fig. 4f), and minor quartz. Sulfides ores are characterized by massive (Fig. 4d), veined (Fig. 4e) and dense disseminated (Fig. 4f) structures, and occurring as subhedral to anhedral granular (Fig. 4h, i), metasomatic (Fig. 4f), enclosed (Fig. 4h), coplanar (Fig. 4g) and interstitial (Fig. 4i) textures. Wall rock alterations including dolomitization, calcitization, silicification, and baritization are common in the Maoping deposit (Xiang et al. 2020). Among which, the dolomitization and silicification are closely related to the Pb–Zn deposits, generally considered as a great pathfinder in exploration for Pb-Zn deposit in the ore district (Wei et al. 2012, 2014, 2015).

3 Sampling and analytical methods

More than ninety representative sulfide ore samples in the Maoping Pb–Zn deposit were collected from the 810, 760, and 720 m adits of the No. I-1 orebody, 720, 670, and 640 m adits of the No. I-2 orebody, 760, and 703 m adits of the No. II orebody. Twenty-nine typical samples were

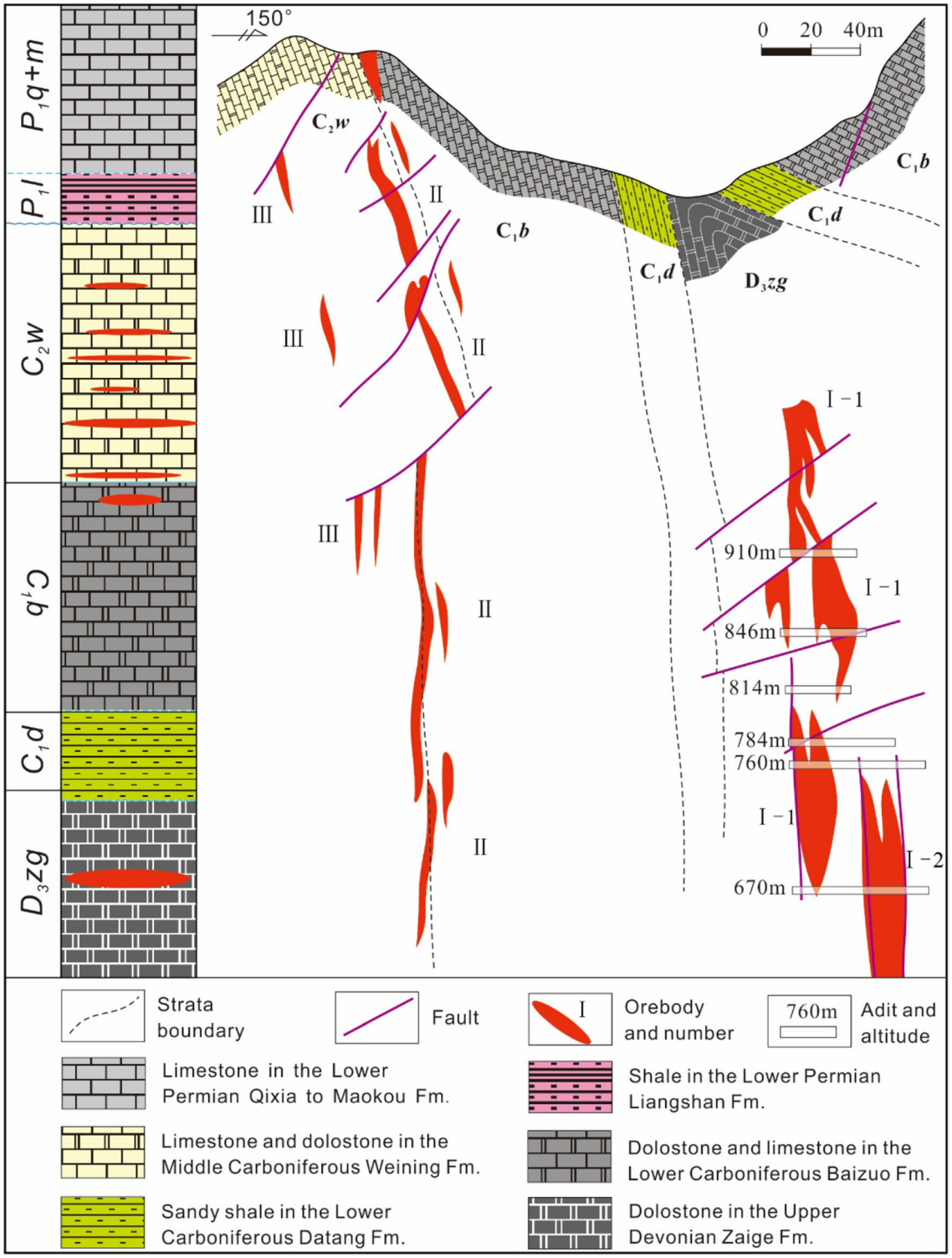

Fig. 3 The comprehensive profile map of the Maoping Pb–Zn deposit, exhibiting the distribution of the orebodies, ore-bearing strata and ore-controlling fault. Modified after Liu and Lin (1999)

crushed into 20 to 60 mesh, and ten ore-stage calcites (seven from No. I and three from No. II orebody) for C–O isotopic analyses, twenty-four sphalerites (thirteen from No. I-1 and eleven from No. I-2 orebody) for S isotopic analysis and fourteen galena samples (eight from No. I-1 and six from No. I-2 orebody) for S-Pb isotopic analyses were hand-picked under a binocular microscope.

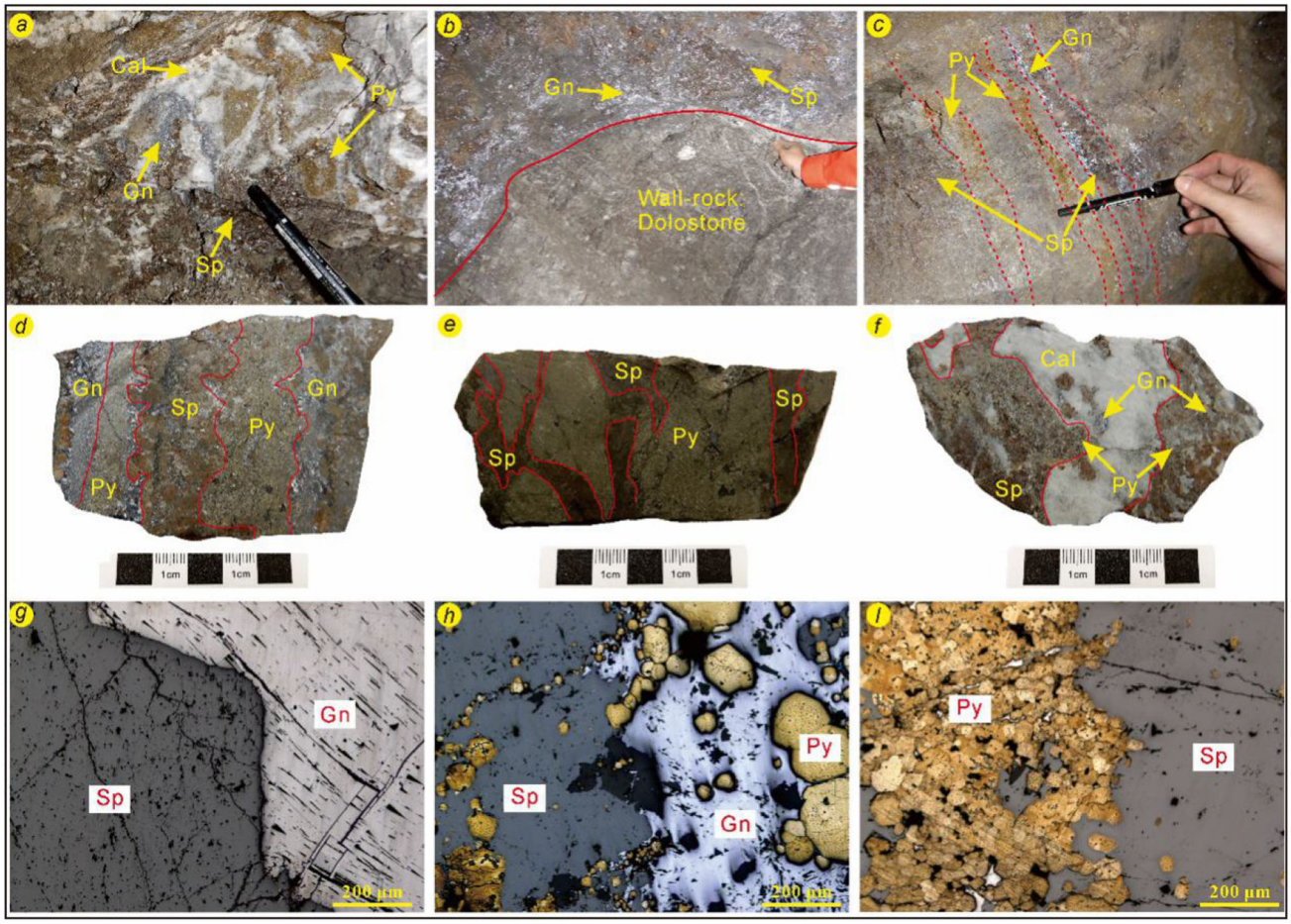

Fig. 4 Photos of the orebodies (**a**–**c**), sulfide samples (**d**–**f**) and microscopic characteristic (**g**–**i**). **a** sulfide minerals (pyrite, sphalerite and galena) replaced and enclosed by calcite; **b** A clear boundary between sphalerite-galena ores and wall rocks (dolostone); **c** Veined pyrite, sphalerite, and galena; **d** Massive sulfide ore including pyrite, sphalerite and galena; **e** Pyrite crosscut and replaced by sphalerite; **f** Dense disseminated sphalerite and galena replaced by calcite; **g** The coexisted sphalerite and galena; **h** pyrite enclosed by sphalerite and galena; **i** The coexisted subhedral sphalerite and pyrite. Abbreviations: Py-pyrite; Sp-sphalerite; Gn-galena; Cal-calcite

The carbon and oxygen isotopic compositions of the ore-stage calcites were performed at the State Key Laboratory of Ore Deposit Geochemistry (SKLODG), Institute of Geochemistry, Chinese Academy of Sciences (IGCAS), determined by a Finnigan MAT-253 mass spectrometer. The analytical precisions (2σ) of $\delta^{13}C$ and $\delta^{18}O$ values were ± 0.2 and ± 0.4 ‰, respectively. The Vienna Pee Dee Belemnite (V-PDB) was considered as standard. $\delta^{18}O_{SMOW} = 1.03086 \times \delta^{18}O_{PDB} + 30.86$ (Friedman and O'Neil 1977).

The sulfur isotopic analysis of the sphalerites and galena was carried out in the SKLODG of the IGCAS, by using the MAT-253 mass spectrometer. The Vienna Canyon Diablo Troilite (V-CDT) was used as a reference standard. IAEA S-1 (− 0.2 ‰), IAEA S-2 (+ 22.6 ‰), and IAEA S-3 (− 32.5 ‰) were regarded as an external standard to correct the isotopic values. The analytical precisions (2σ) of $\delta^{34}S$ values were ± 0.2 ‰.

The lead isotopic analysis of single galena grain was carried out by using the multi-collector inductively coupled plasma mass spectrometry (MC-ICP-MS) at the Radiogenic Isotope Facility of the University of Queensland, Australia. Pb purification procedure and analytical methods for Pb isotopes followed Xun et al. (2014). The measured Pb isotopic compositions of NBS 981 with $^{208}Pb/^{204}Pb$ = 36.7046 ± 140, $^{207}Pb/^{204}Pb$ = 15.4938 ± 38 and $^{206}Pb/^{204}Pb$ = 16.9361 ± 47(n = 38, 2σ) were consistent with that of reported $^{208}Pb/^{204}Pb$ of 36.7179, $^{207}Pb/^{204}Pb$ of 15.4944 and $^{206}Pb/^{204}Pb$ of 16.9410 (Collerson et al. 2002).

4 Results

4.1 Carbon and oxygen isotopic compositions

The C–O isotopic compositions of ten ore-stage calcite samples selected from sulfide ores in the Maoping Pb–Zn deposit are shown in Table 1 and plotted in Fig. 5. The $\delta^{13}C_{PDB}$ and $\delta^{18}O_{SMOW}$ values of calcites from No. I

orebody range from − 5.3 to − 1.7 ‰ (n = 7, mean = − 3.8 ± 1.5 ‰) and + 14.6 to + 21.8 ‰ (n = 7, mean = + 18.9 ± 2.8 ‰), respectively. Calcites from No. II orebody have $\delta^{13}C_{PDB}$ and $\delta^{18}O_{SMOW}$ values varying from − 4.3 to − 0.8 ‰ (n = 3, mean = − 2.7 ± 1.7 ‰) and + 15.1 to + 20.7 ‰ (n = 3, mean = + 18.2 ± 2.8 ‰).

4.2 Sulfur isotopic compositions

The sulfur isotopic compositions of sulfides from the Maoping Pb–Zn deposit are listed in Table 2 and shown in Fig. 6. The $\delta^{34}S_{CDT}$ values of sphalerites and galena from No. I-1 orebody vary from + 13.1 to + 14.9 ‰ (n = 13, mean = + 14.0 ± 0.5 ‰) and + 16.1 to + 19.0 ‰ (n = 6, mean = + 17.7 ± 0.9 ‰), respectively. Sphalerites and galena from No. I-2 orebody have $\delta^{34}S_{CDT}$ values ranging from + 20.1 to 21.8 ‰ (n = 11, mean = + 21.1 ± 0.4 ‰) and + 18.0 to + 19.0 ‰ (n = 5, mean = + 18.3 ± 0.4 ‰).

4.3 Lead isotopic compositions

The lead isotopic compositions of galena from the Maoping Pb–Zn deposit are displayed in Table 3 and plotted in Figs. 7 and 8. The $^{206}Pb/^{204}Pb$, $^{207}Pb/^{204}Pb$ and $^{208}Pb/^{204}Pb$ ratios of seven galena in No. I-1 orebody are 18.729–18.757 (mean = 18.750), 15.773–17.775 (mean = 17.775) and 39.413–39.466 (mean = 39.451), respectively. Six galena from No. I-2 orebody have Pb isotopic ratios with $^{206}Pb/^{204}Pb$ of 18.713–18.759 (mean = 18.746), $^{207}Pb/^{204}Pb$ of 15.772–15.775 (mean = 15.774) and $^{208}Pb/^{204}Pb$ of 39.383–39.467 (mean = 39.440).

5 Discussions

5.1 Sources of CO_2

C–O isotopic system is one of the powerful tools to trace the source(s) of the ore-forming fluid (Zheng and Wang 1991; Carr et al. 1995; Li et al. 2015). The carbon and oxygen in the hydrothermal metallogenic setting are generally derived from mantle ($\delta^{13}C_{PDB}$ = − 8 to − 4 ‰, $\delta^{18}O_{SMOW}$ = + 6 to + 10 ‰; Taylor et al. 1967), marine carbonate rocks ($\delta^{13}C_{PDB}$ = − 4 to + 4 ‰, $\delta^{18}O_{SMOW}$ = + 20 to + 30 ‰; Veizer and Hoefs 1976), and sedimentary organic matter ($\delta^{13}C_{PDB}$ = − 30 to − 10 ‰, $\delta^{18}O_{SMOW}$ = + 24 to + 30 ‰; Demény et al. 1998; Kump and Arthur 1999). Although calcites separated from the Maoping deposit had similar $\delta^{13}C_{PDB}$ values (− 5.3 to − 0.8 ‰) to that of the mantle, its $\delta^{18}O_{SMOW}$ values (+ 14.6 to + 21.8 ‰) are significantly higher than that of the mantle (Fig. 5), suggesting that the mantle possibly contributed minor CO_2 by degassing process of the Emeishan mantle plume (Huang et al. 2004, 2010) but it cannot be a major source of CO_2 in the hydrothermal fluid. These ore-stage calcites have higher $\delta^{13}C_{PDB}$ values and relatively lower $\delta^{18}O_{SMOW}$ values than those of organic matter (Fig. 5), whereas partial data show a slightly negative correlation formed by dehydroxylation of organic matter in the diagram of $\delta^{13}C_{PDB}$ versus $\delta^{18}O_{SMOW}$, indicating that the sedimentary organic matter is a potential CO_2 contributor for hydrothermal fluid. Besides, most calcites have similar $\delta^{13}C_{PDB}$ but relatively lower $\delta^{18}O_{SMOW}$ values than that of marine carbonate rocks (Fig. 5), which may be caused by the carbonate dissolution process that leads to the C isotopes remaining almost constant while O isotopic values decreasing (Banner and Hanson

Table 1 Carbon-Oxygen isotopic compositions of calcite from the Maoping Pb–Zn deposit

Sample no.	Ore bodies	Altitude (m)	$\delta^{13}C_{V\text{-}PDB}$ (‰)	$\delta^{18}O_{V\text{-}SMOW}$ (‰)	Reference
MP-16-15	I	760	− 3.6	+ 15.4	This paper
MP-16-22	I	760	− 1.8	+ 20.9	
MP-16-19	I	760	− 3.7	+ 21.1	
MP-16-27	I	720	− 5.2	+ 14.6	
MP-16-30	I	720	− 5.0	+ 19.5	
MP-16-72	I	720	− 1.7	+ 21.8	
MP-16-63	I	640	− 5.3	+ 19.2	
MP-16-25	II	760	− 0.8	+ 15.1	
MP-16-87	II	760	− 3.2	+ 20.7	
MP-16-65	II	703	− 4.0	+ 18.7	
MPR-286	III	910	− 2.7	+ 17.2	Han et al. (2007)
MPR-82	II	846	− 1.1	+ 18.0	
MPO-5-1	I	846	− 3.7	+ 18.8	

Analysis errors of $\delta^{13}C$ and $\delta^{18}O$ were generally within 0.2 ‰ and 0.4 ‰, respectively

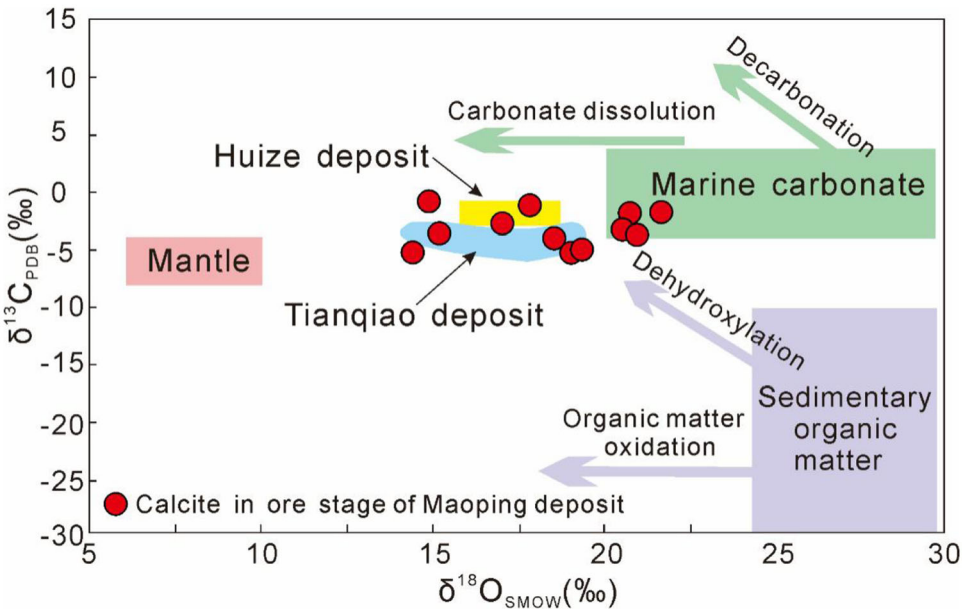

Fig. 5 Plots of $\delta^{13}C_{PDB}$ versus $\delta^{18}O_{SMOW}$ of ore-stage calcites in the Maoping deposit (the fields modified after Liu and Liu 1997). The data of Huize and Tianqiao Pb–Zn deposits are taken from Huang et al. (2010) and Zhou et al. (2013a), respectively

1990). Hence, the origin of CO_2 in the hydrothermal fluid has a closer relationship with the dissolution process of marine carbonate rocks.

The systematic C–O isotopes in this study are similar but more scattered than previous $\delta^{13}C_{PDB}$ (− 3.7 to − 1.1 ‰) and $\delta^{18}O_{SMOW}$ (+ 17.2 to + 18.8 ‰) values (Table 1; Han et al. 2007). The C–O isotopic compositions of calcites in the No. I orebody is consistent with those in the No. II and III orebodies (Table 1), indicating that the different orebodies share the same CO_2 origin in the Maoping deposit. Compared with the $\delta^{13}C_{PDB}$ and $\delta^{18}O_{SMOW}$ values of the Huize (Huang et al. 2004, 2010) and Tianqiao (Zhou et al. 2012, 2013a) Pb–Zn deposit in the SYG region, the C–O isotopic data of the Maoping deposit plot in the similar field to the Huize and Tianqiao deposit (Fig. 5), which may suggest that regional ore-forming fluid have a homologous carbon and oxygen source. We thus consider that a mixture of ternary members that include the dissolution of marine carbonate rocks, the degassing process of the Emeishan mantle plume, and dehydroxylation of sedimentary organic matter could have collectively contributed CO_2 for ore-forming fluids, but the dissolution of marine carbonate rocks was the most significant CO_2 contributor.

5.2 Source of reduced sulfur

The total sulfur isotope composition ($\delta^{34}S_{\Sigma S}$) of ore-forming fluids is essential for tracing sulfur source (Rye and Ohmoto 1974; Ohmoto 1972, 1979). Sulfur generally occurs in the form of sulfides rather than sulfate minerals under the condition of low oxygen fugacity (fo_2) (Pinckney and Rafter 1972). Mineral assemblages mainly consist of sphalerite, galena, pyrite, dolostone, calcite, and quartz with the absence of sulfate minerals in the Maoping deposit, suggesting that $\delta^{34}S_{CDT}$ values of sulfides represent $\delta^{34}S_{\Sigma S}$ of the ore-forming fluid (Ohmoto and Goldhaber 1997). Sulfur isotopic compositions of sulfides (sphalerite and galena) ranging from 13.1 to 21.8 ‰ (n = 35, mean = 17.5 ± 3.0 ‰) are significantly different from mantle-derived sulfur (− 4 to + 8 ‰; Fig. 6; Chaussidon et al. 1989). Hence, basalts formed by the Emeishan mantle plume movement were unlikely to provide sulfur for hydrothermal fluids.

Sulfide samples collected systematically from the No. I-1 and I-2 orebody to constrain the sulfur source(s) of the Maoping deposit. Strikingly different $\delta^{34}S_{CDT}$ values (Table 2) occur among No. I-1 orebody (+ 13.1 to + 19.0 ‰, n = 19, mean = + 15.2 ± 1.8 ‰), No. I-2 orebody (+ 18.03 to + 21.8 ‰, n = 16, mean = 20.2 ± 1.4 ‰), No. II orebody (+ 8.6 to + 17.4 ‰, n = 8, mean = + 12.5 ± 3.1 ‰; Ren et al. 2018), and sulfides in unknown locations of the Maoping deposit (+ 22.5 to + 25.7 ‰, n = 8, mean = + 24.1 ± 1.2 ‰; Tan et al. 2019; Xiang et al. 2020), which may be caused by different sulfur contributors. The $\delta^{34}S_{CDT}$ values of sphalerites (+ 13.1 to + 14.9 ‰) are lower than that of galena (+ 16.1 to + 19.0 ‰) from 720 to 810 m adits of No. I-1 orebody (Table 2; Fig. 6), indicating that the sulfur isotopic fractionation among sulfides did not reach an equilibrium. Conversely, sphalerites with $\delta^{34}S_{CDT}$ values of + 20.1 to + 21.8 ‰ are higher than that of galena (+ 18.0 to + 19.0 ‰) from 720 to 810 m adits of No. I-2 orebody (Table 2; Fig. 6), suggesting an equilibrated S isotopic fractionation among sulfides. This sudden change of S isotopes between No. I-1 orebody over 720 m

Table 2 Sulfur isotopic compositions of sulfides in the Maoping Pb–Zn deposit

Sample no.	Minerals	Altitude	$\delta^{34}S_{V\text{-}CDT}$ (‰)	Ore bodies	Strata	Reference
MP-16-1	Sphalerite	810 m	+ 13.9	I-1		This paper
MP-16-7	Sphalerite	760 m	+ 14.1	I-1		
MP-16-17	Sphalerite	760 m	+ 14.2	I-1		
MP-16-9	Sphalerite	760 m	+ 14.4	I-1		
MP-16-8	Sphalerite	760 m	+ 13.9	I-1		
MP-16-8	Galena	760 m	+ 17.5	I-1		
MP-16-14	Sphalerite	760 m	+ 13.1	I-1		
MP-16-14	Galena	760 m	+ 19.0	I-1		
MP-16-15	Sphalerite	760 m	+ 14.9	I-1		
MP-16-15	Galena	760 m	+ 18.0	I-1		
MP-16-16	Sphalerite	760 m	+ 14.1	I-1	D_3zg	
MP-16-16	Galena	760 m	+ 16.1	I-1		
MP-16-22-1	Sphalerite	760 m	+ 14.6	I-1		
MP-16-22-2	Sphalerite	760 m	+ 14.4	I-1		
MP-16-22	Galena	760 m	+ 17.5	I-1		
MP-16-37-1	Sphalerite	720 m	+ 13.8	I-1		
MP-16-37-2	Sphalerite	720 m	+ 13.8	I-1		
MP-16-37	Galena	720 m	+ 17.9	I-1		
MP-16-32	Sphalerite	720 m	+ 13.4	I-1		
MP-16-75-1	Sphalerite	720 m	+ 21.0	I-2		This paper
MP-16-82	Sphalerite	720 m	+ 21.1	I-2		
MP-16-86	Sphalerite	720 m	+ 21.0	I-2		
MP-16-70	Sphalerite	720 m	+ 20.1	I-2		
MP-16-70	Galena	720 m	+ 19.0	I-2		
MP-16-40	Sphalerite	670 m	+ 21.7	I-2		
MP-16-40	Galena	670 m	+ 18.1	I-2		
MP-16-41	Sphalerite	670 m	+ 21.4	I-2		
MP-16-41	Galena	670 m	+ 18.1	I-2	D_3zg	
MP-16-45	Sphalerite	670 m	+ 21.0	I-2		
MP-16-49	Sphalerite	670 m	+ 21.8	I-2		
MP-16-58	Sphalerite	640 m	+ 21.1	I-2		
MP-16-58	Galena	640 m	+ 18.4	I-2		
MP-16-61-2	Sphalerite	640 m	+ 21.0	I-2		
MP-16-61-3	Sphalerite	640 m	+ 21.0	I-2		
MP-16-61	Galena	640 m	+ 18.0	I-2		
MP940-1-1	Pyrite	940 m	+ 17.4	II		Ren et al. (2018)
MP940-3-1	Pyrite	940 m	+ 12.7	II		
MP940-4-1	Pyrite	940 m	+ 15.3	II		
MP940-3-3	Sphalerite	940 m	+ 11.6	II		
MP940-4-3	Sphalerite	940 m	+ 11.3	II	C_1b	
MP940-5-2	Sphalerite	940 m	+ 14.1	II		
MP940-3-2	Galena	940 m	+ 8.6	II		
MP940-5-1	Galena	940 m	+ 8.8	II		
MP-36-1	Pyrite	Not mentioned	+ 25.7	Not mentioned	Not mentioned	Xiang et al. (2020)
MP-36-2	Pyrite		+ 22.5			
MP-38-1	Pyrite		+ 24.3			
MP-38-2	Pyrite		+ 22.9			

Table 2 continued

Sample no.	Minerals	Altitude	$\delta^{34}S_{V\text{-}CDT}$ (‰)	Ore bodies	Strata	Reference
MP-53-1	Sphalerite	Not mentioned	+ 25.1	Not mentioned	Not mentioned	Tan et al. (2019)
MP-53-2	Sphalerite		+ 24.6			
MP-64-1	Sphalerite		+ 25.1			
MP-64-2	Sphalerite		+ 22.9			

Analysis errors for $\delta^{34}S_{V\text{-}CDT}$ were within 0.2 ‰

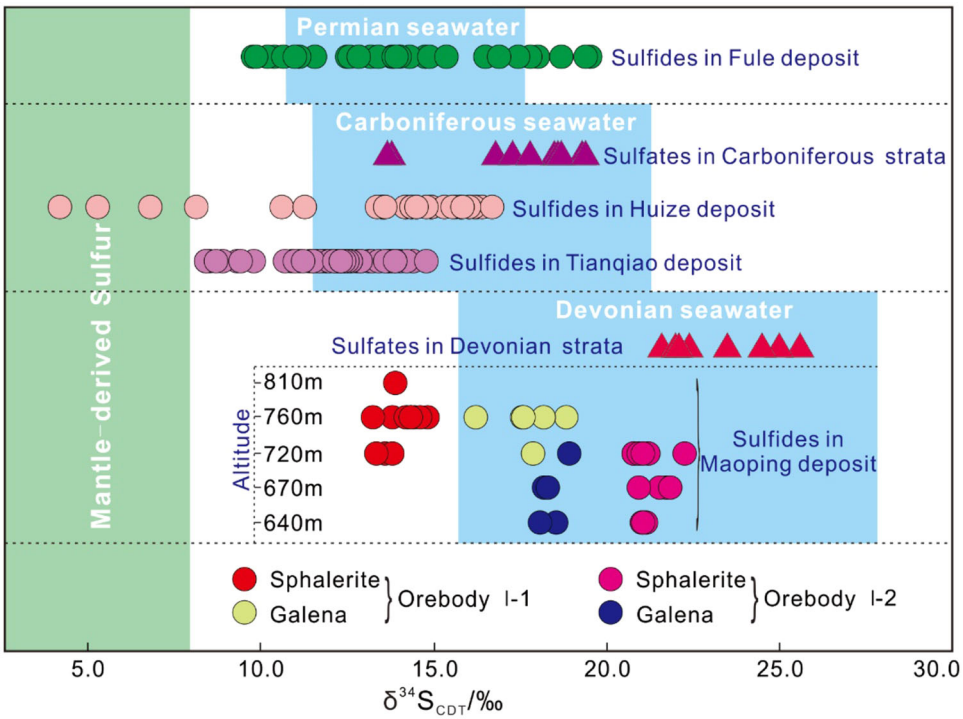

Fig. 6 Comparison of S isotopic compositions of sulfides, sulfates, mantle-derived sulfur and seawater among the Pb–Zn deposits hosted in the different strata in the SYG metallogenic province. Sulfur isotopic data sources: Fule deposit (Zhou et al. 2018), Huize deposit (Li et al. 2007), Tianqiao deposit (Zhou et al. 2014a), sulfates in the Carboniferous and Devonian strata (Ren et al. 2018), seawater in different ages (Claypool et al. 1980) and mantle-derived sulfur (Chaussidon et al. 1989)

($\delta^{34}S_{sphalerite} < \delta^{34}S_{galena}$; Fig. 6) and No. I-2 orebody below 720 m ($\delta^{34}S_{sphalerite} < \delta^{34}S_{galena}$; Fig. 6) demonstrate multiple sulfur reservoirs and complex metallogenic process in the Maoping deposit.

Local sulfate reduction mechanism in the SYG Pb–Zn metallogenic province has been suggested by many researchers (Zhou et al. 2013a; Li et al. 2015; Ren et al. 2018; Tan et al. 2019; Xiang et al. 2020). Previous studies proposed that the sulfur source(s) of the Pb–Zn deposits in the SYG region, such as Nayongzhi hosted in the Cambrian carbonate rocks, Huize hosted in the Carboniferous carbonate rocks and Fule hosted in the Permian carbonate rocks, were derived from evaporites in their ore-bearing strata (Huang et al. 2004; Zhou et al. 2013b, 2014b; Jin et al. 2016; Wang et al. 2017, Luo et al. 2020). The reduced sulfur of No. II orebody (group) that hosted in the Lower Carboniferous Baizuo Formation has been proven to be derived from the thermochemical sulfate reduction (TSR) of the marine sulfates in the ore-bearing strata (Ren et al. 2018), which was supported by suitable temperature (180–218 °C; Han et al. 2007; Liu et al. 2017), the existence of marine evaporites and reduced sulfur reservoir in the ore-hosting strata, implications from sulfur isotopic values of sulfides (+ 18.3 to + 22.7 ‰) and gypsums (+ 21.9 to + 25.9 ‰). However, No. I-1 and I-2 orebodies with different sulfur isotopic compositions and fractionation mechanisms are both hosted in carbonate rocks of the Upper Devonian Zaige Formation. He sulfur isotopic values of No. I-1 orebody (+ 13.1 to + 19.0 ‰) and No. I-2 orebody (+ 18.0 to + 21.8 ‰) in Maoping are respectively consistent with those of Carboniferous marine sulfate minerals (gypsum and barite, + 10.4 ‰ to + 18.6 ‰; Ren et al. 2018) and Devonian marine evaporites (gypsum, + 21.9 to + 25.9 ‰; Ren et al. 2018) in the periphery of

Table 3 Lead isotopic compositions of galena from the Maoping Pb–Zn deposit

Sample no.	Location	$^{208}Pb/^{204}Pb$	± 2σ	$^{207}Pb/^{204}Pb$	± 2σ	$^{206}Pb/^{204}Pb$	± 2σ	Reference
MP-16-8	I-1	39.462	0.002	15.776	0.001	18.757	0.001	This paper
MP-16-9		39.466	0.001	15.776	0.001	18.757	0.001	
MP-16-15		39.461	0.001	15.775	0.001	18.756	0.001	
MP-16-16		39.466	0.001	15.775	0.001	18.757	0.001	
MP-16-17		39.432	0.001	15.774	0.001	18.742	0.001	
MP-16-22		39.460	0.002	15.775	0.001	18.756	0.001	
MP-16-37		39.413	0.001	15.773	0.001	18.729	0.001	
MP-16-40	I-2	39.428	0.001	15.774	0.001	18.740	0.001	This paper
MP-16-41		39.455	0.001	15.774	0.001	18.753	0.001	
MP-16-58		39.467	0.001	15.775	0.001	18.759	0.001	
MP-16-61		39.454	0.001	15.774	0.001	18.754	0.001	
MP-16-70		39.383	0.001	15.772	0.001	18.713	0.001	
MP-16-72		39.455	0.001	15.775	0.001	18.754	0.001	
MP-28-01	II	39.490	0.007	15.790	0.002	18.763	0.002	Tan et al. (2019)
MP-28-02		39.495	0.006	15.791	0.002	18.763	0.002	
MP-28-03		39.484	0.006	15.788	0.002	18.761	0.002	
MP-67-01		39.445	0.006	15.789	0.002	18.740	0.002	
MP-67-02		39.447	0.006	15.788	0.002	18.739	0.002	
MP-67-03		39.467	0.008	15.795	0.003	18.746	0.003	
MP-33-01	II	39.530	0.006	15.801	0.002	18.772	0.002	Xiang et al. (2020)
MP-33-02		39.526	0.008	15.802	0.003	18.773	0.003	
MP-35-01		39.480	0.006	15.789	0.002	18.759	0.002	
MP-35-02		39.484	0.007	15.787	0.003	18.762	0.003	
MP-68-01		39.460	0.007	15.793	0.002	18.743	0.002	
MP-68-02		39.444	0.006	15.788	0.002	18.739	0.002	
MP-71-01		39.475	0.008	15.797	0.003	18.750	0.003	
MP-71-02		39.446	0.007	15.788	0.002	18.738	0.002	

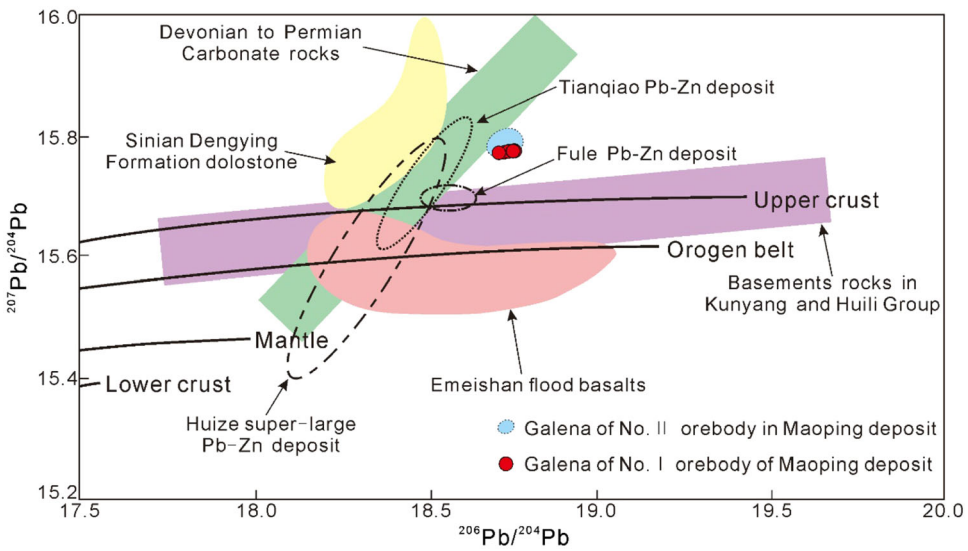

Fig. 7 Plots of $^{207}Pb/^{204}Pb$ versus $^{206}Pb/^{204}Pb$ of galena in the Maoping Pb–Zn deposit (fields modified after Zartman and Doe 1981). Pb isotopic compositions sources: Huize deposit (Huang et al. 2004), Tianqiao deposit (Zhou et al. 2013a), galena of No. II orebody in the Maoping deposit (Tan et al. 2019; Xiang et al. 2020), Devonian to Permian carbonate rocks, Sinian Dengying Formation dolostone, basement rocks in the Kunyang and Huili Group and Emeishan flood basalts (Huang et al. 2004)

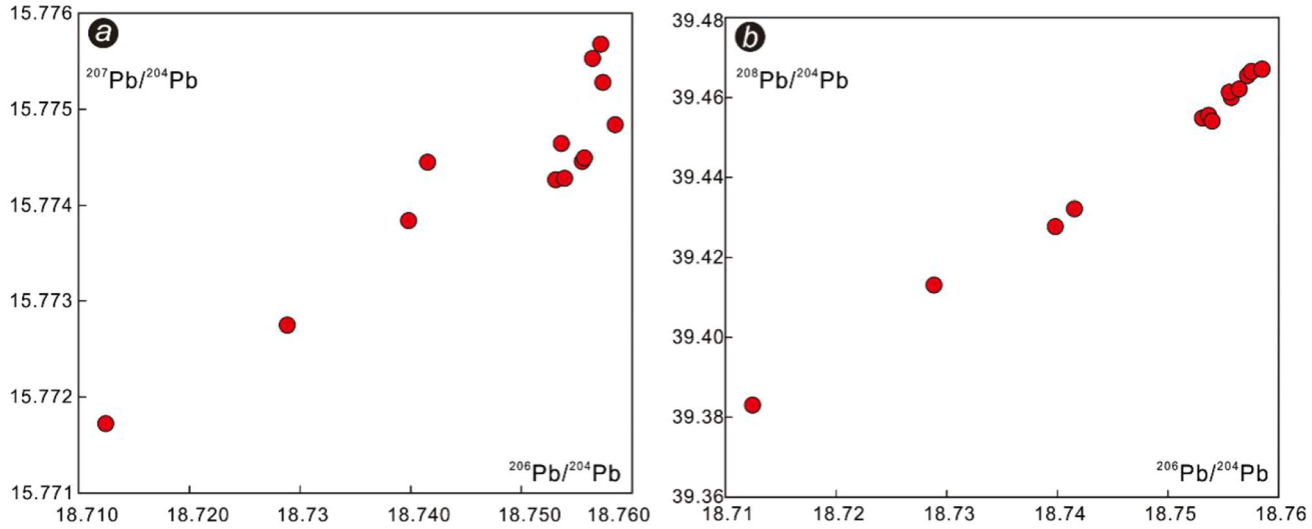

Fig. 8 Plots of $^{207}Pb/^{204}Pb$ versus $^{206}Pb/^{204}Pb$ (**a**) and $^{208}Pb/^{204}Pb$ versus $^{206}Pb/^{204}Pb$ (**b**) of galena in No. I orebody for the Maoping deposit

ore district (Fig. 6). Hence, we consider that the overlying Carboniferous sulfates leached by hydrothermal fluids were transported to ore-hosting strata, and then TSR took place under the action of organic matter to generate reduced sulfur reservoirs for No. I-1 orebody. The reduced sulfur of the No. I-2 orebody should come from the local TSR of evaporites in the Upper Devonian Zaige Formation.

5.3 Source of metals

The Pb isotopic compositions of sulfides are considered approximately equal to that of ore-forming fluids owing to the contents of U and Th in those sulfides are too low to generate corresponding radiogenic Pb isotopes (Carr et al. 1995; Zhou et al. 2001; Gao et al. 2020). The homogeneous Pb isotopic ratios with $^{206}Pb/^{204}Pb$ of 18.713–18.759, $^{207}Pb/^{204}Pb$ of 15.772–15.776, and $^{208}Pb/^{204}Pb$ of 39.383–39.467 from No. I orebody analyzed by single galena grain are similar to those in situ Pb isotopic compositions ($^{206}Pb/^{204}Pb$ = 18.738–18.773, $^{207}Pb/^{204}Pb$ = 15.787–15.802 and $^{208}Pb/^{204}Pb$ = 39.444–39.530) from No. II orebody determined by MC-LA-ICPMS (Fig. 7; Tan et al. 2019; Xiang et al. 2020), suggesting that both the bulk and in situ analyses obtained accurate Pb isotopic data and all orebodies had an identical metal source in the Maoping deposit. This narrow and uniform Pb isotopic signature also indicates a single or well-mixed metal source(s) in the Maoping deposit.

Sinian to Middle Permian ore-hosting sedimentary rocks, Proterozoic Kunyang and Huili Group basements rocks and Late Permian Emeishan continental flood basalts are collectively regarded as three potential metal source rocks for Pb–Zn deposits in the SYG region (Liu and Lin 1999; Huang et al. 2004; Zhou et al. 2018). Until now, the lack of accurate metallogenic age for the Maoping Pb–Zn deposit limits the understanding of the source and evolution of ore-forming fluids. Orebodies of the Maoping deposit hosted in the interlayer fracture zone of the Maomaoshan anticline in which the oldest strata are Permian ($\sim$ 250 Ma), which thus suggests that the Pb–Zn mineralization should be later than 250 Ma. Also, the main metallogenic age of 230–200 Ma was universally recognized for Pb–Zn deposits in the Upper Yangtze region (Li et al. 2007; Zhang et al. 2015; Hu et al. 2016, 2017b), whereas the Emeishan basalts were formed at 260 Ma ago (Zhou et al. 2002; Xu et al. 2004). Hence, it was hard for Emeishan basaltic rocks to contribute metals for Maoping deposit, which was also supported by Pb isotopic ratios plotting above the average upper crustal Pb evolution curves (Zartman and Doe, 1981) and remaining far away from that of the age-corrected (200 Ma; Xiang et al. 2020) Emeishan basalts (Fig. 7).

In the diagram of $^{207}Pb/^{204}Pb$ versus $^{206}Pb/^{204}Pb$ (Fig. 7), the Pb isotopic ratios of galena in Maoping plot between those age-corrected (200 Ma, Xiang et al. 2020) basement metamorphic rocks and ore-bearing carbonate rocks but much closer to the latter, which indicate a mixed rather than single metal source for ore-forming fluids. Furthermore, all Pb isotopic ratios distributing in a steep linear trend (Fig. 8) also indicate that the metals may have been derived from a well-mixed source of different Pb end-members (Carr et al. 1995; Ding et al. 2016). Thus, this study tends to suggest that the ore-forming metals for the Maoping deposit were mainly derived from the Devonian to Permian sedimentary rocks with a certain contribution from the Proterozoic Kunyang and Huili Group basement rocks.

5.4 Ore genesis

Controversies about the ore genesis of the Maoping deposit are mainly on epigenetic sedimentation-reworking (Liu and Lin 1999), strata-bound (Han et al. 2007; Hu 2004), hydrothermal reworking sedimentation-exhalative (SEDEX) (Wang et al. 2009) and MVT (Zhang et al. 2005) Pb–Zn deposit. The characteristics of epigenetic hydrothermal mineralization in the Maoping deposit are strongly supported by the fault-fold ore-controlling system (Figs. 1, 2, 3), the occurrence of orebodies (Fig. 4a–c), ore fabrics (Fig. 4d–i) and isotopic features (Figs. 5, 6, 7). The multilayered Pb–Zn metallogenesis in carbonate rocks of the D_3zg, C_1b, and C_2w indicates that the origin of the Maoping deposit is not a syn-sedimentary or SEDEX.

The Maoping deposit has many similar features with those typical MVT Pb–Zn deposit, such as the tectonic setting (carbonate platform), ore-hosting carbonate rocks (dolostone and limestone; Figs. 3, 4), common wall-rock alteration (dolomitization, calcitization, and silicification; Fig. 4), simple mineral assemblage (sphalerite, galena, pyrite, dolostone, calcite, and quartz; Fig. 4), fault-fold-lithology ore-controlling factors (Figs. 2, 3), marine sulfate as a sulfur contributor (Fig. 6), and metal sources from basements and sedimentary rocks (Fig. 7). However, differences also exist between the Maoping and typical MVT deposit as follow: (1) the Maoping deposit was spatially located in the ELIP (Fig. 1b; Huang et al. 2004; Li et al. 2007), while the typical MVT deposit usually has little relationship with magmatism (Leach et al. 2005, 2010); (2) fluid inclusions features (180–218 °C, 4.1–9.5 wt% NaCl equiv.; Zhang et al. 2015; Liu et al. 2017) are different from those (50–250 °C, 10–30 wt% NaCl equiv.) of MVT (Leach et al. 2005, 2010); and (3) high grades (12–30 wt% Pb + Zn) of sulfide ores is inconsistent with that (av. Pb + Zn < 10 wt%) of the typical MVT Pb–Zn deposit (Leach et al. 2005, 2010). Zhang et al. (2019a, b) proposed that the high grades of sulfide ores in the SYG region was caused by relatively low pH of the ore-forming fluid (pH < 3.6; Zhang et al. 2017), stronger driving forces to transport large-scale hydrothermal fluid (Han et al. 2012, 2014), and a high degree of earlier formed hydroxides [$Pb(OH)_2$ and $Zn(OH)_2$] converting into stable sulfides. Besides, the formation of a large amount of H_2O was also associated with the conversion of hydroxides into sulfides, which was likely to dilute the ore-forming fluid resulting in a decrease in salinity. Hence, the similarities and differences between the Maoping and MVT Pb–Zn deposit indicate the particularity and complexity of the mineralization for Maoping deposit, which may be closely related to the local geological background, chemical conditions (pH, temperature, salinity), driving forces of transport, degree of hydrolysis, and redox conditions (Zhang et al. 2019a, b). But these particularities and complexities cannot deny that the genetic type of the Maoping deposit belongs to an MVT-like Pb–Zn deposit.

6 Conclusions

(1) The CO_2 in ore-forming fluids was generated by the dissolution of marine carbonate rocks, degassing process of the Emeishan mantle plume, and dehydroxylation of sedimentary organic matter.

(2) Like other Pb–Zn deposits in the SYG region, the reduced sulfur of the Maoping deposit was mainly produced by TSR of marine evaporites within the ore-bearing strata, but the reduced sulfur of the No. I-1 orebody hosted in the Upper Devonian Zaige Formation may have been contributed by marine sulfate in the overlying Carboniferous strata.

(3) The ore-forming fluid in the Maoping deposit has a mixed metal source involving the Devonian to Permian sedimentary rocks and the Proterozoic Kunyang and Huili Group basement rocks with the absent contribution of the Late Permian Emeishan basalts.

(4) The Maoping deposit is an MVT-like Pb–Zn deposit.

Acknowledgements This research project was supported by the National Natural Science Foundation of China (Grant Nos. U1812402 and 41673056). We would like to thank Engineer Jing Gu and Engineer Jing Hu for the assistance in isotopic analyses. We are also indebted to the Yiliang Chihong Mining Co., Ltd for their permission to investigate and sample the Maoping deposit. We are grateful to Prof. Haifeng Fan and Prof. Yongyong Tang for the thoughtful comments. Their constructive and stimulating suggestions helped to significantly improve the manuscript.

References

Banner JL, Hanson GN (1990) Calculation of simultaneous isotopic and trace element variations during water rock interaction with applications to carbonate diagenesis. Geochim Cosmochim Acta 54:3123–3137

Carr GR, Dean JA, Suppel DW, Heithersay PS (1995) Precise lead isotope fingerprinting of hydrothermal activity associated with Ordovician to Carboniferous metallogenic events in the Lachlan fold belt of New South Wales. Econ Geol 90(6):1467–1505

Chaussidon M, Albarède F, Sheppard SMF (1989) Sulphur isotope variations in the mantle from ion microprobe analyses of micro-sulphide inclusions. Earth Planet Sci Lett 92(2):144–156

Chen SH, Han RS, Shentu LY, Wu P, Qiu WL, Wen DX (2016) Alteration zoning and geochemical element migration in alteration rock of Zhaotong lead-zinc deposit in northeastern yunnan mineralization concentration area. J Jilin Univ (Earth Sci Ed) 46(3):711–721 **(in Chinese with English abstract)**

Claypool GE, Holser WT, Kaplan IR, Sakai H, Zak I (1980) The age curves of sulfur and oxygen isotopes in marine sulfate and their mutual interpretation. Chem Geol 28:199–260

Collerson KD, Kamber BS, Schoenberg R (2002) Applications of accurate, high-precision Pb isotope ratio measurement by multi-collector ICP-MS. Chem Geol 188(1–2):65–83

Cui JH, Han RS (2014) Ore-forming fluid evidence of Zhaotong Zn–Pb deposit genesis in the Zn–Pb deposit concentrated district of northeast Yunnan. Min Resour Geol 1:18–24 **(in Chinese with English abstract)**

Demény A, Ahijado A, Casillas R, Vennemann TW (1998) Crustal contamination and fluid/rock interaction in the carbonatites of Fuerteventura (Canary Islands, Spain): a C, O. H isotope study. Lithos 44(3–4):101–115

Ding T, Ma DS, Lu JJ, Zhang RQ, Zhang ST (2016) S, Pb, and Sr isotope geochemistry and genesis of Pb–Zn mineralization in the Huangshaping polymetallic ore deposit of southern Hunan Province, China. Ore Geol Rev 77:117–132

Friedman I, O'Neil JR (1977) Compilation of stable isotope fractionation factors of geochemical interest. data of geochemistry, U.S. Geological Survey Professional Paper 440-KK, pp 1–12

Gao RZ, Xue CJ, Chi GX, Dai JF, Dong C, Zhao XB, Man RH (2020) Genesis of the giant Caixiashan Zn-Pb deposit in Eastern Tianshan, NW China: constraints from geology, geochronology and S–Pb isotopic geochemistry. Ore Geol Rev 119:1–18

Han RS, Zou HJ, Hu B, Hu YZ, Xue CD (2007) Features of fluid inclusions and sources of ore-forming fluid in the Maoping carbonate-hosted Zn–Pb–(Ag–Ge) deposit, Yunnan, China. Acta Petrol Sin 23(9):2109–2118 **(in Chinese with English abstract)**

Han RS, Hu YZ, Wang XK, Huang ZL, Chen J (2012) Mineralization model of Rich Ge–Ag-Bearing Zn–Pb polymetallic deposit concentrated district in northeastern Yunnan, China. Acta Geol Sin 86(2):280–294 **(in Chinese with English abstract)**

Han RS, Wang F, Hu YZ, Wang XK, Ren T, Qiu WL et al (2014) Metallogenic tectonic dynamics and chronology constrains on the Huize-Type (HZT) germanium rich silver-zinc-lead deposits. Geotect Metal 38:758–771 **(in Chinese with English abstract)**

Hu B (2004) Features of geology-geochemistry and prognosis of concealed bodies for maoping zinc-lead deposit in zhaotong, yunnan. MSc Dissertation, Kunming University of Science and Technology **(in Chinese with English abstract)**

Hu RZ, Fu SL, Xiao JF (2016) Major scientific problems on low temperature metallogenesis in South China. Acta Petrol Sin 32(11):3239–3251 **(in Chinese with English abstract)**

Hu RZ, Fu SL, Huang Y, Zhou MF, Fu SH, Zhao CH, Wang YJ, Bi XW, Xiao JF (2017a) The giant South China Mesozoic low temperature metallogenic domain: reviews and a new geodynamic model. J Asian Earth Sci 137:9–34

Hu RZ, Chen WT, Xu DR, Zhou MF (2017b) Reviews and new metallogenic models of mineral deposits in South China: an introduction. J Asian Earth Sci 137:1–8

Huang ZL, Chen J, Han RS, Li WB, Liu CQ, Zhang ZL, Ma DY, Gao DR, Yang HL (2004) Geochemistry and ore genesis of the Huize Giant Pb–Zn deposit in Yunnan Province, China: discussion on the relationship between the Emeishan flood basalts and Pb–Zn mineralization. Geological Publishing House, Beijing pp 1–214 **(in Chinese)**

Huang ZL, Li XB, Zhou MF, Li WB, Jin ZG (2010) REE and C–O isotopic geochemistry of calcites from the word-class Huize Pb–Zn deposits, Yunnan, China: implication for the ore genesis. Acta Geol Sin (Engl Ed) 84:597–613

Jin ZG, Zhou JX, Huang ZL, Ye L, Luo K, Gao JG, Chen XL, Wang B, Peng S (2016) Ore genesis of the Nayongzhi Pb–Zn deposit, Puding city, Guizhou Province, China: evidences from S and in situ Pb isotopes. Acta Petrol Sin 32(11):3441–3455 **(in Chinese with English abstract)**

Kump LR, Arthur MA (1999) Interpreting carbon-isotope excursions: carbonates and organic matter. Chem Geol 161:181–198

Leach DL, Sangster D, Kelley KD, Large RR, Garven G, Allen C, Gutzmer J, Walters S (2005) Sediment-hosted lead-zinc deposits: a global perspective. In: Economic geology 100th Anniversary, Lancaster, PA: Economic Geology Publishing Co. pp 561–607

Leach DL, Bradley DC, Huston D, Pisarevsky SA, Taylor RD, Gardoll SJ (2010) Sediment-hosted lead-zinc deposits in Earth history. Econ Geol 105(3):593–625

Li B, Zhou JX, Huang ZL, Yan ZF, Bao GP, Sun HR (2015) Geological, rare earth elemental and isotopic constraints on the origin of the Banbanqiao Zn–Pb deposit, Southwest China. J Asian Earth Sci 111:100–112

Liu HC, Lin WD (1999) Regularity research of lead-zinc-silver deposits in northeastern Yunnan Province. Kunming: Yunnan University Press, pp 1–468 **(in Chinese)**

Liu JM, Liu JJ (1997) Basin fluid genetic model of sediment-hosted microdisseminated gold deposits in the gold-triangle area between Guizhou, Guangxi and Yunnan. Acta Mineral Sinica 17: 448-456 **(in Chinese with English abstract)**

Liu WH, Zhang J, Wang J (2017) Sulfur isotope analysis of carbonate-hosted Zn–Pb deposits in northwestern Guizhou Province, Southwest China: implications for the source of reduced sulfur. J Geochem Explor 181:31–44

Li WB, Huang ZL, Yin MD (2007) Dating of the giant Huize Zn-Pb ore field of Yunnan province, southwest China; constraints from the Sm-Nd system inhydrothermal calcite. Resour Geol 57:90–97

Luo K, Zhou JX, Huang ZL, Caufeld J, Zhao JX, Feng YX, Ouyang HG (2020) New insights into the evolution of Mississippi Valley-Type hydrothermal system: a case study of the Wusihe Pb–Zn deposit, South China, using quartz in situ trace elements and sulfides in situ S–Pb isotopes. Am Min 105:35–51

Ohmoto H (1972) Systematics of sulfur and carbon isotopes in hydrothermal ore deposits. Econ Geol 67(5):551–579

Ohmoto H (1979) Isotope of sulfur and carbon. Geochem Hydrotherm Ore Depos:509–567

Ohmoto H, Goldhaber MB (1997) Sulfur and carbon isotopes. In: Barnes HL (ed) Geochemistry of hydrothermal ore deposits, 3rd edn. Wiley, New York, pp 517–611

Pinckney DM, Rafter TA (1972) Fractionation of sulfur isotopes during ore deposition in the Upper Mississippi Valley zinc-lead district. Econ Geol 67(3):315–328

Qiu WL, Bo Li, Shentu LY (2013) The trace elements geochemical characteristics of sphalerite in Zhaotong lead-zinc deposits. Sci Technol Eng 13(18):5282–5286 **(in Chinese with English abstract)**

Ren SL, Li YH, Zeng PS, Qiu WL, Fan CF, Hu GY (2018) Effect of Sulfate evaporate salt layer in mineralization of the Huize and Maoping lead-zinc deposits in Yunnan: evidence from sulfur isotope. Acta Geol Sin 92(5):1041–1055 **(in Chinese with English abstract)**

Rye RO, Ohmoto H (1974) Sulfur and carbon isotopes and ore genesis: a review. Econ Geol 69(6):826–842

Shen ZW, Jin CH, Dai YP, Zhang Y, Zhang H (2016) Mineralization age of the Maoping Pb–Zn deposit in the northeastern Yunnan Province: evidence from Rb–Sr isotopic dating of sphalerites. Geol J China Univ 22(2):213–218 **(in Chinese with English abstract)**

Tan SC, Zhou JX, Li B, Zhao JX (2017) In situ Pb and bulk Sr isotope analysis of the Yinchanggou Pb–Zn deposit in Sichuan Province (SW China): constraints on the origin and evolution of hydrothermal fluids. Ore Geol Rev 91:432–443

Tan SC, Zhou JX, Luo K, Xiang ZZ, He HH, Zhang YH (2019) The sources of ore-forming elements of the Maoping Large-Scale Pb–Zn deposit, Yunnan Province: constrains from in situ S and

Pb isotopes. Acta Petrol Sin 35:3461–3476 **(in Chinese with English abstract)**

Taylor HP Jr, Frechen J, Degens ET (1967) Oxygen and carbon isotope studies of carbonatites from the Laacher See District, West Germany and the Alnö District Sweden. Geochim Cosmochim Acta 31(3):407–430

Veizer J, Hoefs J (1976) The nature of $^{18}O/^{16}O$ and $^{13}C/^{12}C$ secular trends in sedimentary carbonate rocks. Geochimca et Cosmochimica Acta 40(11):1387–1395

Wang CW, Yuan LI, Luo HY, Liu XL (2009) Genesis of Maoping Pb–Zn deposit in Yunnan province. J Kunming Univ Sci Technol 34(1):7–11 **(in Chinese with English abstract)**

Wang JW, An ZZ, Wen GJ (2017) Geological characteristics comparison and exploration prospective analyses of lead-zinc deposit in heba area of Maoping in yiliang and yunlu of weining. Guizhou Geol 34(3):160–168 **(in Chinese with English abstract)**

Wang LJ, Mi M, Zhou JX, Luo K (2018) New constraints on the origin of the Maozu carbonate-hosted epigenetic Zn-Pb deposit in NE Yunnan Province, SW China. Ore Geol Rev 101:578–594

Wei AY, Xue CD, Hong T, Luo DF, Li LL, Wang F, Zhou GM, Liu X (2012) The alteration-mineralization zoning model for the Maoping lead-zinc deposit, northeastern Yunnan province: evidence from alternation-lithofacies mapping. Acta Petrologica et Mineralogica 31(5):723–735 **(in Chinese with English abstract)**

Wei AY, Xue CD, Li J, Liu X (2014) Alteration, order degree and geochemistry features of dolomites associated with Zinc-Lead mineralization in Maoping Pb–Zn deposit, NE Yunnan, China. Acta Geol Sin (Engl Ed) 88(supp. 2):217–218

Wei AY, Xue CD, Xiang K, Li J, Liao C, Akhter QJ (2015) The ore-forming process of the Maoping Pb–Zn deposit, northeastern Yunnan, China: constraints from cathodoluminescence (cl) petrography of hydrothermal dolomite. Ore Geol Rev 70:562–577

Xiang ZZ, Zhou JX, Lou K (2020) New insights into the multi-layer metallogenesis of carbonated-hosted epigenetic Pb–Zn deposits: a case study of the Maoping Pb–Zn deposit, South China. Ore Geol Rev 122:1–16

Xu YG, He B, Chung SL, Menzies MA, Frey FA (2004) Geologic, geochemical and geophysical consequences of plume involvement in the Emeishan flood-basalt province. Geology 32:917–920

Xun W, Xu YG, Feng YF, Zhao JX (2014) Plume-lithosphere interaction in the generation of the Tarim Large Igneous Province, NW China: geochronological and geochemical constraints. Am J Sci 314:314–356

Yang Q, Liu W, Zhang J, Wang J, Zhang X (2019) Formation of Pb–Zn deposits in the Sichuan–Yunnan–Guizhou triangle linked to the Youjiang foreland basin: evidence from Rb–Sr age and in situ sulfur isotope analysis of the Maoping Pb–Zn deposit in northeastern Yunnan Province, southeast China. Ore Geol Rev 107:780–800

Ye L, Cook NJ, Ciobanu CL, Liu YP, Zhang Q, Liu TG, Gao W, Yang YL, Danyushevsky L (2011) Trace and minor elements in sphalerite from base metal deposits in South China: a LA-ICPMS study. Ore Geol Rev 39(4):188–217

Zartman RE, Doe BR (1981) Plumbotectonics: the model. Tectonophysics 75(1–2):135–162

Zhang CQ, Mao JW, Wu SP, Li HM, Liu F, Guo BJ, Gao DR (2005) Distribution, characteristics and genesis of Mississippi Valley Type lead-zinc deposits in Sichuan–Yunnan–Guizhou area. Min Depos 24(3):336–348 **(in Chinese with English abstract)**

Zhang CQ, Wu Y, Hou L, Mao JW (2015) Geodynamic setting of mineralization of Mississippi Valley-type deposits in world-class Sichuan–Yunnan–Guizhou Zn–Pb triangle, southwest China: implications from age-dating studies in the past decade and the Sm-Nd age of the Jinshachang deposit. J Asian Earth Sci 103:103–114

Zhang Y, Han R, Wei P, Qiu W (2017) Fluid inclusion features and physicochemical conditions of the Kuangshanchang Pb–Zn Deposit, Huize, Yunnan Province. J Jilin Univ 47:719–733 **(in Chinese with English abstract)**

Zhang HJ, Fan HF, Xiao CY, Wen HJ, Ye L, Huang ZL, Zhou JX, Guo QJ (2019a) The mixing of multi-source fluids in the Wusihe Zn–Pb ore deposit in Sichuan Province, Southwestern China. Acta Geochim 38(5):642–653

Zhang Y, Han RS, Ding X, Wang YR, Wei PT (2019b) Experimental study on fluid migration mechanism related to Pb–Zn super-enrichment: implications for mineralization mechanisms of the Pb–Zn deposits in the Sichuan–Yunnan–Guizhou, SW China. Ore Geol Rev 114:1–19

Zheng MH, Wang XC (1991) Ore genesis of the Daliangzi Pb–Zn deposit in Sichuan, China. Econ Geol 86(4):831–846

Zhou CX, Wei CS, Guo JY (2001) The source of metals in the Qilingchang Pb–Zn deposit, northeastern Yunnan, China: Pb–Sr isotope constraints. Econ Geol 96(3):583–598

Zhou MF, Malpas J, Song XY, Robinson PT, Sun M, Kennedy AK, Esher CM, Keays RR (2002) A temporal link between the Emeishan large igneous province (SW China) and the end Guadalupian mass extinction. Earth Planet Sci Lett 196:113–122

Zhou JX, Huang ZL, Zhuo GF, Zeng QS (2012) C, O isotope and REE geochemistry of the hydrothermal calcites from the Tianqiao Pb–Zn ore deposit in NW Guizhou Province, China. Geotectonica et Metallogenia 36(1):93–101 **(in Chinese with English abstract)**

Zhou JX, Huang ZL, Zhou MF, Li XB, Jin ZG (2013a) Constraints of C–O–S–Pb isotope compositions and Rb–Sr isotopic age on the origin of the Tianqiao carbonate-hosted Pb–Zn deposit, SW China. Ore Geol Rev 53:77–92

Zhou JX, Huang ZL, Bao GP, Gao JG (2013b) Sources and thermochemical sulfate reduction for reduced sulfur in the hydrothermal fluids, southeastern SYG Pb–Zn metallogenic province, SW China. J Earth Sci 24(5):759–771

Zhou JX, Huang ZL, Zhou MF, Zhu XK, Muchez P (2014a) Zinc, sulfur and lead isotopic variations in carbonate-hosted Pb–Zn sulfide deposits, Southwest China. Ore Geol Rev 58:41–54

Zhou JX, Huang ZL, Lü ZC, Zhu XK, Gao JG, Mirnejad H (2014b) Geology, isotope geochemistry and ore genesis of the Shanshulin carbonate-hosted Pb–Zn deposit, Southwest China. Ore Geol Rev 63:209–225

Zhou JX, Luo K, Wang XC, Wilde SA, Wu T, Huang ZL, Cui YL, Zhao JX (2018) Ore genesis of the Fule Pb–Zn deposit and its relationship with the Emeishan Large Igneous Province: evidence from mineralogy, bulk C–O–S and in situ S–Pb isotopes. Gondwana Res 54:161–179

Zhu CW, Wen HJ, Zhang YX, Fu SH, Fan HF, Cloquet C (2017) Cadmium isotope fractionation in the Fule Mississippi Valley-type deposit, Southwest China. Miner Depos 52(5):675–686

Zou HJ, Han RS, Hu B, Liu H (2004) New evidences of origin of metallogenic materials in the Maoping Pb–Zn ore deposit, Zhaotong, Yunnan: r-factor analysis results of trace elements in NE-extending fractural tectonites. Geol Prospect 40:43–48 **(in Chinese with English abstract)**